Chapter 5
Molecular Mechanisms for Ion Transportation of Microbial Rhodopsins Studied by Light-Induced Difference FTIR Spectroscopy

Yuji Furutani

Abstract Microbial rhodopsins, many variants of which were developed via genetic engineering, have been widely utilized as optogenetic tools. Understanding the molecular mechanisms is important for designing such tools more efficiently. The dynamics of these proteins upon photoactivation can be studied by light-induced difference Fourier transform infrared (FTIR) spectroscopy. As the structural information involves hydrogen, which is not readily accessible via X-ray crystallography, light-induced difference FTIR spectroscopy is a powerful tool to study the molecular mechanisms of these light-receptive proteins. Low-temperature and time-resolved FTIR spectroscopy on two major microbial rhodopsins—bacteriorhodopsin (BR) and halorhodopsin (HR)—are summarized in this review. The low-temperature method stabilizes the intermediate states by decreasing temperature, whereas the time-resolved method allows direct observation at physiological temperature by using a measurement time short enough for their detection. By measuring the difference spectra in X–H and X–D stretching regions, changes in the hydrogen-bonding networks, including water molecules, were elucidated. It was demonstrated that water molecules played an important role in proton and ion translocation in BR and HR. Therefore, for develop optogenetic tools with favorable molecular properties, it may be important to design protein structures in the presence of internal water molecules.

Keywords Vibrational spectroscopy • Bacteriorhodopsin • Halorhodopsin • Hydrogen bonds • Water molecules • Light energy

Y. Furutani (✉)
Department of Life and Coordination-Complex Molecular Science, Institute for Molecular Science, Myodaiji, Okazaki 444-8585, Japan

Department of Structural Molecular Science, The Graduate University for Advanced Studies (SOKENDAI), Myodaiji, Okazaki 444-8585, Japan

PRESTO, Japan Science and Technology Agency (JST),
4-1-8 Honcho, Kawaguchi, Saitama 332-0012, Japan
e-mail: furutani@ims.ac.jp

H. Yawo et al. (eds.), *Optogenetics*, DOI 10.1007/978-4-431-55516-2_5

5.1 Introduction

Optogenetic tools (Deisseroth 2011; Boyden 2011; Fenno et al. 2011; Bernstein and Boyden 2011) developed from microbial rhodopsins, such as channelrhodopsin (ChR) (activation of nerve cells), halorhodopsin (HR), bacteriorhodopsin (BR), and archerhodopsin (silencing of nerve cells), have played important roles in the initial phases of this field of research. ChR is widely used in optogenetics, due to its ability to activate neurons of interest in vitro and in vivo by focusing laser or light-emitting diode (LED) light, which increases spatiotemporal resolution relative to the conventional electrode method. Various derivatives of ChR have been developed by introducing site-specific mutations and making chimera of ChRs from different clades in the phylogenetic tree. The molecular mechanisms employed in the light-gated channel and light-driven ion pumps of microbial rhodopsins are not well understood, despite the availability of the atomic structural data. Many physicochemical researchers are therefore investigating the molecular mechanisms of rhodopsin molecules, primarily for their potential to innovate and improve the function of optogenetic tools. This review article summarizes how the molecular mechanisms of microbial rhodopsins have been elucidated, particularly focusing on studies using infrared spectroscopic techniques.

5.2 The Difference Infrared Spectroscopy for Analyzing Light-Induced Structural Changes in Microbial Rhodopsins

The three-dimensional atomic structural information of proteins can be obtained by X-ray crystallography, nuclear magnetic resonance (NMR) spectroscopy, and electron microscopy. The spatial resolution achieved by these methods is 0.1–10 nm, depending on the experimental techniques and conditions. The structural models are visualized by a molecular modeling software such as PyMOL used in this review. Microbial rhodopsin is a transmembrane protein with seven α-helices spanning the membrane. The crystallization of membrane proteins is generally considered more difficult than soluble proteins. Many X-ray crystal structures of microbial rhodopsins have been elucidated in the past quarter of a century. Through the development of crystallization techniques using microbial rhodopsins, the lipidic cubic phase method was developed (Rummel et al. 1998) and has become a standard method for the crystallization of membrane proteins (e.g., G-protein-coupled receptors [GPCRs]). In 2012, the X-ray crystal structure of ChR was resolved, with important implications for research in the optogenetic field (Kato et al. 2012).

Although various intermediate states of microbial rhodopsins have been analyzed via X-ray crystallography, especially for BR (Lanyi 2004; Pebay-Peyroula et al. 2000), it has been challenging to elucidate the active state that induces the

large protein conformational changes coupled with the protein function, such as channel gating or ion transportation. For example, visual rhodopsin in crystal lattice forms a yellow species like metarhodopsin II, wherein the large conformational change of helix six was not observed in the crystal (Salom et al. 2006). The formation of the crystal lattice may in fact impair conformational changes of a protein that take place in physiological conditions (Efremov et al. 2006). Time-resolved X-ray measurements triggered by a pulsed laser light have been successfully applied in the picosecond time range (Srajer et al. 1996) to capture the ultrafast phenomenon of photoreceptive proteins, such as a *cis-trans* photo-isomerization of chromophore (Schotte et al. 2012). Although structural changes important for expression of protein functions take place in the micro-to-millisecond time range, they may be hampered by crystal packing (Efremov et al. 2006). Spectroscopic and infrared spectroscopic methods with sufficient time resolution have been used to detect protein conformational changes. Light-induced difference infrared spectroscopy, which calculates a difference spectrum between infrared spectra obtained before and after the photoreaction, has been employed to analyze structural changes of BR (Maeda 2001; Kandori 2000; Heberle 2000; Gerwert 1999; Siebert 1995; Rothschild 1992) and other microbial rhodopsins (Furutani and Kandori 2014; Furutani et al. 2008, 2005). The molecular mechanisms of microbial rhodopsins have been investigated by combining spectroscopic data with the static atomic structures of the proteins produced predominantly by X-ray crystallography.

A photon of infrared light has an equivalent energy to that of a molecular vibration. Therefore, infrared absorption spectra give us information about chemical bonds, such as C–C single bonds and C=C double bonds in a retinal molecule. Rhodopsin has a retinal molecule as the chromophore, which primarily comprises an ethylenic chain with alternate C–C and C=C bonds. Photoisomerization of the retinal chromophore changes the frequencies of C–C and C=C stretching vibrations, as observed in light-induced difference infrared spectra (Fig. 5.1; the lower side). Protein is a polymer composed of 20 types of amino acids connected by peptide bonds. The primary structure is the sequence of the amino acids, which provides secondary and tertiary structures through the protein-folding reactions. α helices and β sheets are typical secondary protein structures that are formed by hydrogen bonds between C=O and N–H groups on a peptide backbone. Amide I and II bands are observed in an infrared spectrum of protein (Fig. 5.1; the upper side). The amide I band in particular is generally utilized for analysis of secondary protein structures (Barth and Zscherp 2002). Amino acid side chains also show vibrational bands in their typical frequency regions (Barth 2000). Among them, the C=O stretching bond of a protonated carboxylate group of aspartic and glutamic acids residues appearing in the frequency region of 1,780–1,700 cm^{-1} has been utilized as an indicator of the protonation states in microbial rhodopsins.

Water strongly absorbs infrared light, disturbing the measurement of infrared absorption spectra of protein in the solution. Therefore, the thickness of a sample cell for infrared spectroscopy is limited to several micrometers; alternatively, a protein film formed on an infrared window is used for the measurement.

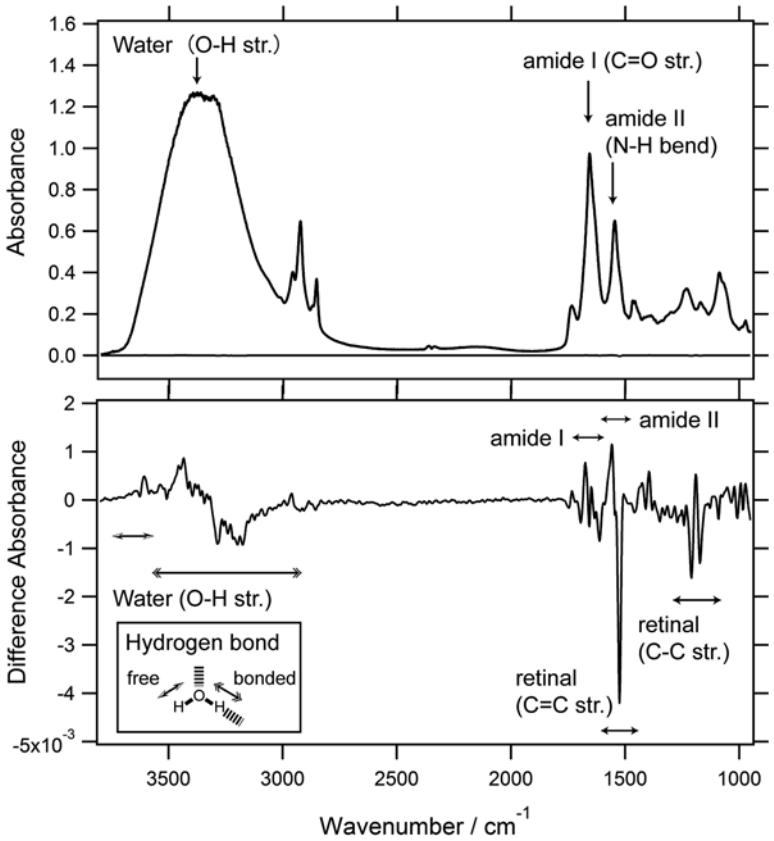

Fig. 5.1 An infrared absorption spectrum of *Natronomonas pharaonis* halorhodopsin (*Np*HR) in a hydrated film sample (the *upper side*) and its light-induced difference spectrum (the *lower side*). The difference spectrum is also shown in the upper side, yet it appears to be a zero line due to minimal spectral change caused by the photoreaction. The spectral change is attributed to the protein moiety (amide I and II), the retinal chromophore (C–C and C=C str.), and the internal water molecules (O–H str.) in *Np*HR

A dried protein film is favorable for measurement of infrared absorption spectra; however, protein molecules under such conditions fail to exhibit the proper structural changes observed in hydrated conditions (Nishimura et al. 1995). Considering this dilemma, the amount of water in protein samples should be carefully regulated. By appropriately reducing water content in the sample, O–H and O–D stretching vibrations of water molecules inside proteins can be observed (Furutani et al. 2005; Maeda 2001; Kandori 2000). By doing so, we can understand changes in the hydrogen bonds of water molecules in protein, which is considered to be a remarkable advantage of difference infrared spectroscopy (Fig. 5.1; the lower side).

5.3 Light-Driven Proton-Pumping Rhodopsin, Bacteriorhodopsin

BR was discovered in 1971 (Oesterhelt and Stoeckenius 1971) and has since been investigated using various experimental and theoretical methods. BR binds an all-*trans* retinal as the choromophore (λ_{max} = 570 nm) and its photoisomerization to the 13-*cis* form occurs within 0.5 ps. Subsequently, several intermediate states of BR, called K, L, M, N, and O, are transiently formed (Lanyi 1993). During the transition from the N to the O state, the 13-*cis* chromophore thermally isomerizes to the all-*trans* form, and the O state returns to the original state. BR pumps a proton in each photocyclic reaction, which takes approximately 10 ms. The proton transfer reactions of BR have been extensively investigated by light-induced difference infrared spectroscopy, which revealed that the first proton transfer step involved deprotonation of the protonated Schiff base and protonation of the counter ion Asp85 upon the formation of the M intermediate (Braiman et al. 1991). After the protein's conformational change, the Schiff base can accept a proton from Asp96, which locates in the extracellular side and donates a proton on the formation of the N intermediate (Pfefferle et al. 1991). Moreover, time-resolved and low-temperature Fourier transform infrared (FTIR) spectroscopy revealed that water clusters play an important role in the proton-transfer processes (Garczarek and Gerwert 2006; Tanimoto et al. 2003).

The proton-transfer process from the Schiff base to Asp85 is a key step for the proton-pumping function of BR, and has been explained by several hypotheses describing changes in the hydrogen-bonding network, including a bridging water molecule. The existence of a water molecule between the Schiff base and Asp85 was suggested via low-temperature FTIR spectroscopy (Maeda et al. 1994) and later confirmed using high-resolution X-ray crystallography (Luecke et al. 1999) (Fig. 5.2). The hydrogen-bond strength of water molecules in each intermediate state has been extensively studied via low-temperature FTIR spectroscopy (Tanimoto et al. 2003; Maeda 2001; Kandori 2000). FTIR revealed that the bridging water has an extremely strong hydrogen bond (O–D stretching vibration at 2,171 cm^{-1}) in the ground state, which changes its strength on formation of the K intermediate (Shibata et al. 2003; Kandori and Shichida 2000) (Fig. 5.3; left). The water is sandwiched between a positive charge on the Schiff base and a negative charge on Asp85. This configuration of the hydrogen-bonding network probably strengthens hydrogen bonds compared with those found in a typical tetrahedral structure in ice according to the previous quantum mechanics/molecular mechanics (QM/MM) result (Hayashi et al. 2004). The QM/MM result also indicated that the light energy was predominantly captured in the retinal distortion, with weakening of the hydrogen bond an additional form of the energy capturing. Interestingly, the hydrogen bond returns to its original strength in the L and M states (Tanimoto et al. 2003) (Fig. 5.3; left). In the M state, Asp85 is protonated; therefore, a possible hydrogen-bonding partner for the water molecule is Asp212, which retains a negative charge in the M state. Based on our interpretation of these experimental results, the hydrogen-bonding switch reaction of the water molecules appears to be a key step for proton transfer reactions from the Schiff base to Asp85 (Fig. 5.3; right).

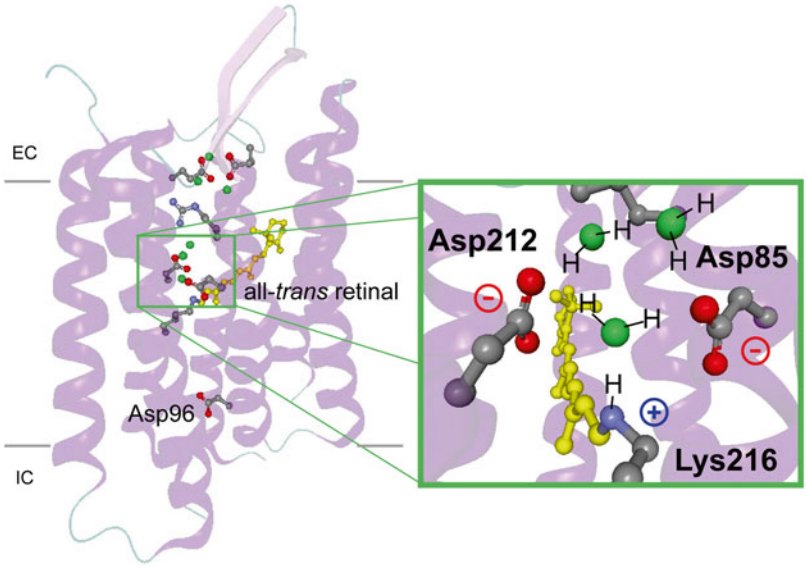

Fig. 5.2 The X-ray crystal structure of bacteriorhodopsin (BR) and the expanded view around the Schiff base region. The extracellular (EC) region is above and the intracellular (IC) region is below. The amino acid residues important for proton-pumping function are depicted

Since the turn of the century, many microbial rhodopsins have been discovered in a diverse variety of organisms; for example, proteorhodopsin, identified in microbacteria living in the ocean, was found to function as a light-driven proton pump and contributes to biomass generation by capturing solar energy (Beja et al. 2000, 2001). Moreover, sodium- (Inoue et al. 2013) and chloride-pumping (Yoshizawa et al. 2014) rhodopsins have also recently been found in the ocean. The molecular mechanisms of these pumping rhodopsins have not as yet been very well studied in comparison with BR. However, comparative studies of these microbial rhodopsins will provide us with a better understanding of their molecular mechanisms for pumping protons, and chloride and sodium ions. In the case of proton pumping, a water molecule with a strong hydrogen bond may be a crucial component (Furutani et al. 2005). From the extensive low-temperature FTIR studies available on many microbial rhodopsins, such water molecules were found in microbial rhodopsins that possess proton-pumping functions.

5.4 Light-Driven Chloride-Pumping Rhodopsin, Halorhodopsin

HR pumps extracellular chloride ions into the cell through a photocyclic reaction similar to that in BR (Varo 2000). Incorporation of chloride ions causes a negative membrane potential and suppresses depolarization of the cell. Therefore, HR,

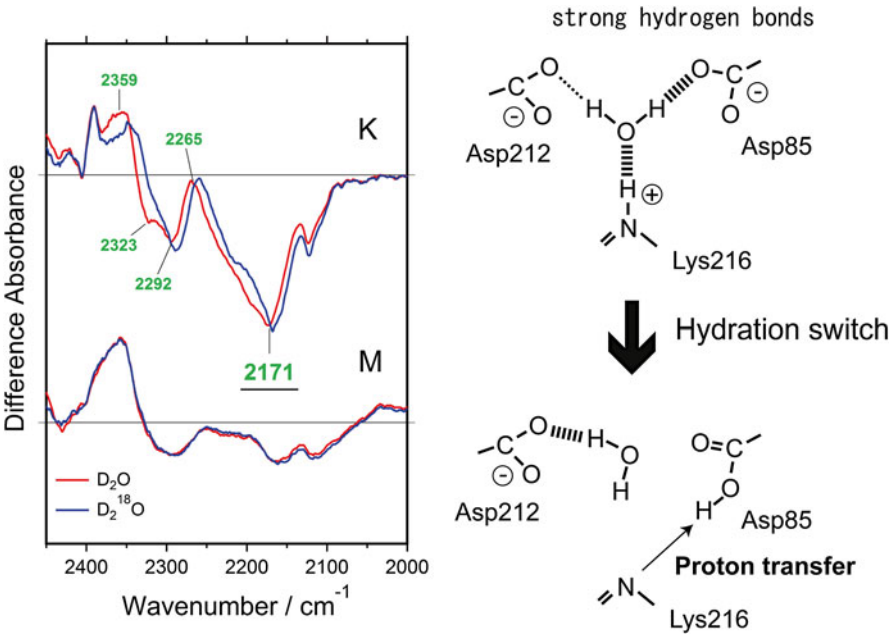

Fig. 5.3 The light-induced difference spectra of bacteriorhodopsin (BR) in the X–D stretching vibration in the 2,450–2,000 cm^{-1} region (*left*) and the proposed model of the initial proton transfer reaction in BR (hydration switch model) (*right*). The *green*-tagged bands were assigned to O–D stretching vibrations of internal water molecules in BR. The lowest band at 2,171 cm^{-1} was also assigned to the N–D stretching vibration of the Schiff base. The hydrogen bonds of the water molecules are weakened at the K intermediate and restore their strength at the M intermediate. On the basis of the experimental result, the model for the initial proton-transfer reaction is depicted

especially from *Natronomonas pharaonis* (*Np*HR), has been utilized as an optogenetic tool to silence action potentials in neurons (Zhang et al. 2007).

HR has an all-*trans* retinal as the chromophore, with an absorption maximum of approximately 580 nm. Photoisomerization of the retinal triggers the photocyclic reaction, where several intermediate states (K, L_1, L_2, N, and O) are formed (Varo 2000). Contrary to in BR, the protonated Schiff base retains its proton during the photocyclic reaction. BR has two negatively charged residues around the Schiff base (Asp85 and Asp212), whereas HR has one aspartate (Asp252 in *Np*HR) and a neutral threonine residue (Thr126 in *Np*HR) at the equivalent position of Asp85 in BR, which facilitates chloride ion binding. Mutation of Asp85 to Thr in BR is known to convert the proton pump to a chloride pump (Sasaki et al. 1995), making Asp85 in BR a crucial residue for determining types of ion pumps. In contrast, the inverse conversion of chloride-pumping function of HR to that of a proton pump by mutagenesis has not yet been successful, although HR can pump protons in the presence of azide molecules (Lakatos et al. 2002).

A chloride ion is a monoatomic ion, with no infrared absorption. Therefore, infrared spectroscopy cannot directly detect a chloride ion in HR. This is in clear contrast to the case of protons in BR. A proton exists as an oxonium ion in an

aqueous solution, or binds to amino acid residues (e.g., Asp, Glu, and His) in protein. Transient protonation and deprotonation of the amino acid residues and water molecules enables us to develop a deep insight into the molecular mechanism behind the proton-pumping function of BR. Although a chloride ion cannot form a chemical bond in HR, it influences the hydrogen-bonding network and ionic interactions with amino acid residues and water molecules. Such slight effects caused by movement of a chloride ion in HR may be detected by infrared spectroscopy. In addition to chloride ions, HR can pump bromide, iodide, and nitrate ions. Comparison of infrared spectroscopic data obtained with these transportable ions was used to elucidate specific ion–protein interactions of water molecules and amino acid residues in HR (Shibata et al. 2005).

The molecular mechanism of HR has been investigated by various physicochemical methods and the X-ray crystal structures in the ground (Kouyama et al. 2010; Kolbe et al. 2000) (Fig. 5.4) and intermediate states (Nakanishi et al. 2013; Gmelin et al. 2007) solved with atomic resolution. The most important process of the HR chloride–pump reaction is the movement of a chloride ion bound near the Schiff base. The first X-ray crystal structure of the HR L_1 intermediate detected a chloride ion in the same position (Gmelin et al. 2007) and indicated that the chloride ion moves in the subsequent intermediate states (L_2 or N state). Previous low-temperature infrared spectroscopy studies also supported the observation and suggested that changes in hydrogen-bonding and the movement of water molecules around the chloride ion in K and L_1 states reduced polarity and hydrophilicity of the environment; thus, promoting movement of the chloride ion into the later intermediate states (Shibata et al. 2005).

In 2012, time-resolved FTIR spectroscopy on *Np*HR, in the entire mid-infrared region, revealed water molecule dynamics of water molecules inside the protein in accordance with protein conformational changes in L_1, L_2, N, and O intermediate states (Furutani et al. 2012). O–H stretching vibrations of water molecules were detected in a >3,600 cm^{-1} region, where the O–H groups were considered not to form hydrogen bonds. The difference in absorption spectra of the O–H stretching vibrations changed little in L_1 and L_2 intermediates but changed more significantly in the N and O states (Furutani et al. 2012) (Fig. 5.5). Based on the X-ray crystal structure, there are three water molecules near the chloride ion in the Schiff base region (Kouyama et al. 2010). The water molecules must change the hydrogen-bonding network when the chloride ion moves inside the cell after formation of the L_1 state. The O–H stretching vibration of water may be an intrinsic probe for chloride ion movement; therefore, the large spectral change of O–H stretching vibrations suggested that the chloride ion moves on formation of the N state. In the O state, the absence of a chloride ion may increase the number of water O–H groups free from a hydrogen bond, as shown by the large positive band in the difference spectra. In the future, when the signal-to-noise ratio in the lower frequency region (3,500–3,000 cm^{-1}) of difference spectra is improved, O–H stretching vibrations of water molecules and Thr residues, which directly interact with the chloride ion, will be more easily detected; thus, increasing our understanding of the molecular mechanism of chloride pumps.

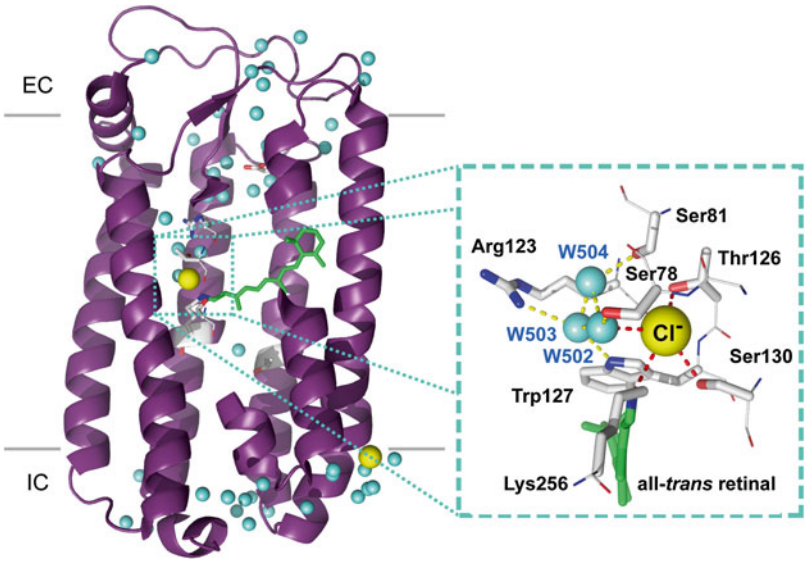

Fig. 5.4 X-ray crystal structure of *Natronomonas pharaonis* halorhodopsin (*Np*HR) and the expanded view around the Schiff base region. The extracellular (EC) side is shown at the *top* and the intracellular (IC) side at the *bottom*. The amino acid residues and water molecules surrounding the initial chloride-binding site are depicted

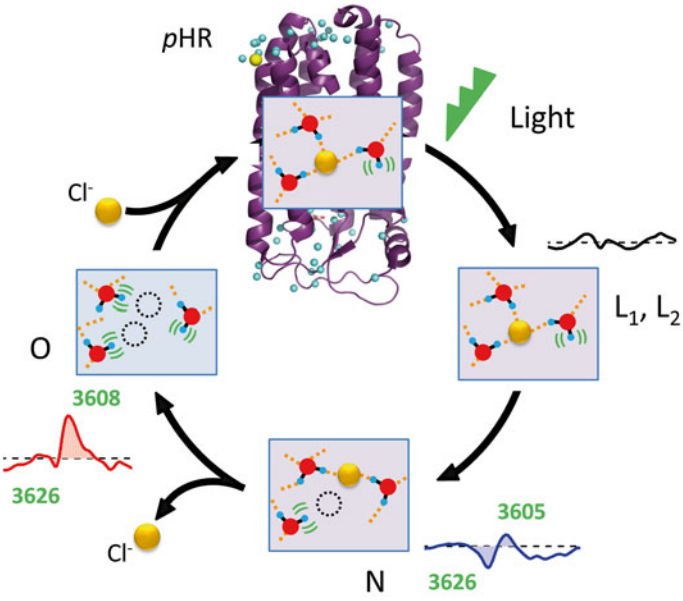

Fig. 5.5 Structural changes of water molecules during the photocyclic reaction of *Natronomonas pharaonis* halorhodopsin (*Np*HR) revealed by time-resolved Fourier transform infrared (FTIR) spectroscopy. Spectral changes of O–H stretching vibrations of water molecules without a hydrogen bond are shown for each intermediate state. It was demonstrated that translocation and release of a chloride ion induced larger spectral changes of water in the N and O intermediate states of *Np*HR

5.5 Light-Gated Ion Channel, Channelrhodopsin

ChR-1 and -2 were originally discovered in the green alga, *Chlamydomonas reinhardtii* (Nagel et al. 2003, 2002). Both function as light-gated cation channels, yet with different ion selectivity. Due to the enhanced electrophysiological properties of ChR-2 (ChR2) in various kinds of cell, it has been widely used as an optogenetic tool for activating neuronal cells by illumination with blue light. ChR2 binds an all-*trans* retinal as the chromophore (λ_{max} = ~470 nm) and with a similar photocyclic reaction to BR and HR. The intermediate states are called P_1 (500 nm), P_2 (390 nm), P_3 (520 nm), and P_4 (480 nm) states (Ritter et al. 2008; Bamann et al. 2008). Among them, the P_3 state is considered an active state where cations pass through ChR2. P_4 has a long lifetime (τ = ~20 s) and is considered to be a desensitized state as determined by electrophysiological measurement. In 2012, the X-ray crystal structure of a chimera of channelrhodpsin-1 and -2 (called C1C2) which was composed of the 1st–5th helices from ChR1 and the 6th–7th helices from ChR2, was revealed (Kato et al. 2012). Prior to the crystallographic study, light-induced difference spectroscopy was applied to ChR2, and elucidated structural changes of Glu90 and conformational changes of protein at 80 and 293 or 298 K (Radu et al. 2009; Ritter et al. 2008). Time-resolved FTIR measurement, with ~10 ms time resolution, was initially applied to ChR2, revealing the kinetics of its conformational changes and the deprotonation of Glu90 in P_3 and P_4 states (Eisenhauer et al. 2012). In early studies, low-temperature and time-resolved methods, with rapid scan mode, were applied to analyze structural changes in the intermediate and photostationary states. Due to the slow recovery kinetics of ChR2 caused by the P_4 intermediate, it was difficult to apply time-resolved FTIR spectroscopy with step-scan mode (reaching higher time resolutions: up to ~ μs), which required more than several hundred repetitive measurements. A pioneering work was reported in 2013 (Lorenz-Fonfria et al. 2013) that revealed conformational changes of the protein with the time constants and transient protonation changes of Glu90 and Asp156. Moreover, the time-resolved measurement exposed the proton transfer reaction from the Schiff base to Glu253, located at the equivalent position of Asp212 in BR. The protonation changes during the photocycle of ChR2 clearly differed from those in BR and HR. Therefore, there are likely to be key events that induce conformational changes of the channel and open the gate. Recently, a low-temperature FTIR study on C1C2 in the X–D stretching region characterized the water-containing hydrogen-bonding network around the Schiff base region (Ito et al. 2014). The study showed that the Schiff base interacts directly with Glu162 (Glu123 in ChR2), forming a strong hydrogen bond with it, while a water molecule formed a strong hydrogen bond with Asp292 (Asp253 in ChR2 and Asp212 in BR). The unique hydrogen-bonding network around the Schiff base region in ChR may be correlated with the unique protein structural changes on photoreaction. Interestingly, the distinctive structural changes of Glu129 (Glu90 in ChR2) in chimeric ChRs compared with that of ChR2 was recently revealed by a light-induced difference FTIR study (Inaguma et al. 2015).

5.6 Conclusion

Light-induced difference FTIR spectroscopy is a powerful tool to study structural changes of microbial rhodopsins. X–H and X–D stretching vibrations provide particularly fruitful information on dynamics of hydrogen-bonding networks inside proteins involved in the ion-pumping reactions, which is usually difficult to be accessed by other physicochemical methods. It was suggested that water molecules probably play an important role in transporting protons and ions inside proteins. Atomic structures determined by structural biological methods such as X-ray crystallography provide the basis of understanding of the molecular mechanisms of proteins; however, it is important to understand what happens to the structural dynamics of the protein when the protein is functioning. Understanding the molecular mechanisms of microbial rhodopsins would be helpful to design optogenetic tools with favorable molecular properties.

Acknowledgments The author thanks many collaborators, especially Professor Hideki Kandori, for studies in this review article and the research grants from KAKENHI (22770159, 22018030, 21023014, 21026016) and JST PRESTO 'Chemical conversion of light energy'. The authors would like to thank Enago (www.enago.jp) for the English language review.

References

Bamann C, Kirsch T, Nagel G et al (2008) Spectral characteristics of the photocycle of channelrhodopsin-2 and its implication for channel function. J Mol Biol 375(3):686–694. doi:10.1016/j.jmb.2007.10.072

Barth A (2000) The infrared absorption of amino acid side chains. Prog Biophys Mol Biol 74(3–5):141–173. doi:10.1016/S0079-6107(00), 00021-3 [pii]

Barth A, Zscherp C (2002) What vibrations tell us about proteins. Q Rev Biophys 35(4):369–430. doi:10.1017/S0033583502003815

Beja O, Aravind L, Koonin EV et al (2000) Bacterial rhodopsin: evidence for a new type of phototrophy in the sea. Science 289(5486):1902–1906

Beja O, Spudich EN, Spudich JL et al (2001) Proteorhodopsin phototrophy in the ocean. Nature 411(6839):786–789. doi:10.1038/35081051

Bernstein JG, Boyden ES (2011) Optogenetic tools for analyzing the neural circuits of behavior. Trends Cogn Sci 15(12):592–600. doi:10.1016/j.tics.2011.10.003, 00216-6 [pii]

Boyden ES (2011) A history of optogenetics: the development of tools for controlling brain circuits with light. Biol Rep 3:11. doi:10.3410/B3-11, 11 [pii]

Braiman MS, Bousche O, Rothschild KJ (1991) Protein dynamics in the bacteriorhodopsin photocycle: submillisecond Fourier transform infrared spectra of the L, M, and N photointermediates. Proc Natl Acad Sci U S A 88(6):2388–2392

Deisseroth K (2011) Optogenetics. Nat Methods 8(1):26–29. doi:10.1038/nmeth.f.324, nmeth.f.324 [pii]

Efremov R, Gordeliy VI, Heberle J et al (2006) Time-resolved microspectroscopy on a single crystal of bacteriorhodopsin reveals lattice-induced differences in the photocycle kinetics. Biophys J 91(4):1441–1451. doi:10.1529/biophysj.106.083345

Eisenhauer K, Kuhne J, Ritter E et al (2012) In channelrhodopsin-2 Glu-90 is crucial for ion selectivity and is deprotonated during the photocycle. J Biol Chem 287(9):6904–6911. doi:10.1074/jbc.M111.327700

Fenno L, Yizhar O, Deisseroth K (2011) The development and application of optogenetics. Annu Rev Neurosci 34:389–412. doi:10.1146/annurev-neuro-061010-113817

Furutani Y, Kandori H (2014) Hydrogen-bonding changes of internal water molecules upon the actions of microbial rhodopsins studied by FTIR spectroscopy. Biochim Biophys Acta 1837(5):598–605. doi:10.1016/j.bbabio.2013.09.004

Furutani Y, Shibata M, Kandori H (2005) Strongly hydrogen-bonded water molecules in the Schiff base region of rhodopsins. Photochem Photobiol Sci 4(9):661–666. doi:10.1039/b416698a

Furutani Y, Sudo Y, Kandori H (2008) FTIR studies of protein-protein interaction changes between pharaonis phoborhodopsin and its cognate transducer protein. Curr Top Biochem Res 10(2):63–77

Furutani Y, Fujiwara K, Kimura T et al (2012) Dynamics of dangling bonds of water molecules in pharaonis halorhodopsin during chloride ion transportation. J Phys Chem Lett 3(20):2964–2969. doi:10.1021/Jz301287n

Garczarek F, Gerwert K (2006) Functional waters in intraprotein proton transfer monitored by FTIR difference spectroscopy. Nature 439(7072):109–112. doi:10.1038/nature04231, nature04231 [pii]

Gerwert K (1999) Molecular reaction mechanisms of proteins monitored by time-resolved FTIR-spectroscopy. Biol Chem 380(7–8):931–935. doi:10.1515/Bc.1999.115

Gmelin W, Zeth K, Efremov R et al (2007) The crystal structure of the L1 intermediate of halorhodopsin at 1.9 angstroms resolution. Photochem Photobiol 83(2):369–377. doi:10.1562/2006-06-23-RA-947

Hayashi S, Tajkhorshid E, Kandori H et al (2004) Role of hydrogen-bond network in energy storage of bacteriorhodopsin's light-driven proton pump revealed by ab initio normal-mode analysis. J Am Chem Soc 126(34):10516–10517. doi:10.1021/Ja047506s

Heberle J (2000) Proton transfer reactions across bacteriorhodopsin and along the membrane. Biochim Biophys Acta 1458(1):135–147, 00064-5 [pii]

Inaguma A, Tsukamoto H, Kato HE et al (2015) Chimeras of channelrhodopsin-1 and -2 from Chlamydomonas reinhardtii exhibit distinctive light-induced structural changes from channelrhodopsin-2. J Biol Chem 290(18):11623–11634. doi:10.1074/jbc.M115.642256

Inoue K, Ono H, Abe-Yoshizumi R et al (2013) A light-driven sodium ion pump in marine bacteria. Nat Commun 4:1678. doi:10.1038/ncomms2689

Ito S, Kato HE, Taniguchi R et al (2014) Water-containing hydrogen-bonding network in the active center of channelrhodopsin. J Am Chem Soc 136(9):3475–3482. doi:10.1021/ja410836g

Kandori H (2000) Role of internal water molecules in bacteriorhodopsin. Biochim Biophys Acta 1460(1):177–191, 00138-9 [pii]

Kandori H, Shichida Y (2000) Direct observation of the bridged water stretching vibrations inside a protein. J Am Chem Soc 122(47):11745–11746. doi:10.1021/Ja0032069

Kato HE, Zhang F, Yizhar O et al (2012) Crystal structure of the channelrhodopsin light-gated cation channel. Nature 482(7385):369–374. doi:10.1038/nature10870

Kolbe M, Besir H, Essen LO et al (2000) Structure of the light-driven chloride pump halorhodopsin at 1.8 A resolution. Science 288(5470):1390–1396, 8554 [pii]

Kouyama T, Kanada S, Takeguchi Y et al (2010) Crystal structure of the light-driven chloride pump halorhodopsin from Natronomonas pharaonis. J Mol Biol 396(3):564–579, doi:S0022-2836(09)01455-7 [pii]

Lakatos M, Groma GI, Ganea C et al (2002) Characterization of the azide-dependent bacteriorhodopsin-like photocycle of salinarum halorhodopsin. Biophys J 82(4):1687–1695. doi:10.1016/S0006-3495(02)75521-5

Lanyi JK (1993) Proton translocation mechanism and energetics in the light-driven pump bacteriorhodopsin. Biochim Biophys Acta 1183(2):241–261

Lanyi JK (2004) X-ray diffraction of bacteriorhodopsin photocycle intermediates. Mol Membr Biol 21(3):143–150. doi:10.1080/09687680410001666345

Lorenz-Fonfria VA, Resler T, Krause N et al (2013) Transient protonation changes in channelrhodopsin-2 and their relevance to channel gating. Proc Natl Acad Sci U S A 110(14):E1273–E1281. doi:10.1073/pnas.1219502110

Luecke H, Schobert B, Richter HT et al (1999) Structure of bacteriorhodopsin at 1.55 A resolution. J Mol Biol 291(4):899–911. doi:10.1006/jmbi.1999.3027, S0022-2836(99)93027-9 [pii]

Maeda A (2001) Internal water molecules as mobile polar groups for light-induced proton translocation in bacteriorhodopsin and rhodopsin as studied by difference FTIR spectroscopy. Biochem Biokhimiia 66(11):1256–1268

Maeda A, Sasaki J, Yamazaki Y et al (1994) Interaction of aspartate-85 with a water molecule and the protonated Schiff base in the L intermediate of bacteriorhodopsin: a Fourier-transform infrared spectroscopic study. Biochemistry 33(7):1713–1717

Nagel G, Ollig D, Fuhrmann M et al (2002) Channelrhodopsin-1: a light-gated proton channel in green algae. Science 296(5577):2395–2398. doi:10.1126/science.1072068

Nagel G, Szellas T, Huhn W et al (2003) Channelrhodopsin-2, a directly light-gated cation-selective membrane channel. Proc Natl Acad Sci U S A 100(24):13940–13945. doi:10.1073/pnas.1936192100

Nakanishi T, Kanada S, Murakami M et al (2013) Large deformation of helix F during the photoreaction cycle of Pharaonis halorhodopsin in complex with azide. Biophys J 104(2):377–385. doi:10.1016/j.bpj.2012.12.018

Nishimura S, Sasaki J, Kandori H et al (1995) Structural changes in the lumirhodopsin-to-metarhodopsin I conversion of air-dried bovine rhodopsin. Biochemistry 34(51):16758–16763

Oesterhelt D, Stoeckenius W (1971) Rhodopsin-like protein from the purple membrane of Halobacterium halobium. Nat New Biol 233(39):149–152

Pebay-Peyroula E, Neutze R, Landau EM (2000) Lipidic cubic phase crystallization of bacteriorhodopsin and cryotrapping of intermediates: towards resolving a revolving photocycle. Biochim Biophys Acta 1460(1):119–132

Pfefferle JM, Maeda A, Sasaki J et al (1991) Fourier transform infrared study of the N intermediate of bacteriorhodopsin. Biochemistry 30(26):6548–6556

Radu I, Bamann C, Nack M et al (2009) Conformational changes of channelrhodopsin-2. J Am Chem Soc 131(21):7313–7319. doi:10.1021/ja8084274

Ritter E, Stehfest K, Berndt A et al (2008) Monitoring light-induced structural changes of Channelrhodopsin-2 by UV-visible and Fourier transform infrared spectroscopy. J Biol Chem 283(50):35033–35041, doi:M806353200 [pii]

Rothschild KJ (1992) FTIR difference spectroscopy of bacteriorhodopsin: toward a molecular model. J Bioenerg Biomembr 24(2):147–167

Rummel G, Hardmeyer A, Widmer C et al (1998) Lipidic cubic phases: new matrices for the three-dimensional crystallization of membrane proteins. J Struct Biol 121(2):82–91. doi:10.1006/jsbi.1997.3952

Salom D, Lodowski DT, Stenkamp RE et al (2006) Crystal structure of a photoactivated deprotonated intermediate of rhodopsin. Proc Natl Acad Sci U S A 103(44):16123–16128. doi:10.1073/pnas.0608022103

Sasaki J, Brown LS, Chon YS et al (1995) Conversion of bacteriorhodopsin into a chloride ion pump. Science 269(5220):73–75

Schotte F, Cho HS, Kaila VR et al (2012) Watching a signaling protein function in real time via 100-ps time-resolved Laue crystallography. Proc Natl Acad Sci U S A 109(47):19256–19261. doi:10.1073/pnas.1210938109

Shibata M, Tanimoto T, Kandori H (2003) Water molecules in the schiff base region of bacteriorhodopsin. J Am Chem Soc 125(44):13312–13313. doi:10.1021/ja037343s

Shibata M, Muneda N, Sasaki T et al (2005) Hydrogen-bonding alterations of the protonated Schiff base and water molecule in the chloride pump of Natronobacterium pharaonis. Biochemistry 44(37):12279–12286. doi:10.1021/bi050726d

Siebert F (1995) Infrared spectroscopy applied to biochemical and biological problems. Method Enzymol 246:501–526

Srajer V, Teng T, Ursby T et al (1996) Photolysis of the carbon monoxide complex of myoglobin: nanosecond time-resolved crystallography. Science 274(5293):1726–1729

Tanimoto T, Furutani Y, Kandori H (2003) Structural changes of water in the Schiff base region of bacteriorhodopsin: proposal of a hydration switch model. Biochemistry 42(8):2300–2306. doi:10.1021/bi026990d

Varo G (2000) Analogies between halorhodopsin and bacteriorhodopsin. Biochim Biophys Acta 1460(1):220–229, doi:S0005-2728(00)00141-9 [pii]

Yoshizawa S, Kumagai Y, Kim H et al (2014) Functional characterization of flavobacteria rhodopsins reveals a unique class of light-driven chloride pump in bacteria. Proc Natl Acad Sci U S A 111(18):6732–6737. doi:10.1073/pnas.1403051111

Zhang F, Wang LP, Brauner M et al (2007) Multimodal fast optical interrogation of neural circuitry. Nature 446(7136):633–639. doi:10.1038/nature05744